Energy Advances

ROYAL SOCIETY OF CHEMISTRY

PAPER

View Article Online
View Journal | View Issue

Cite this: *Energy Adv.*, 2022, 1, 1021

A highly effective zinc-methanesulfonic acid catalyst for acetylene hydration

Sudi Zhang, Qinqin Wang,* Zhen Chen and Bin Dai*

Received 6th October 2022,
Accepted 21st October 2022

DOI: 10.1039/d2ya00272h

rsc.li/energy-advances

Acetylene hydration to acetaldehyde is considered a valuable and potential production route in the acetylene chemical industry. A new Zn-based catalyst was synthesized using a simple method and evaluated for the acetylene hydration reaction. All catalysts were characterized by XRD, BET, TGA, TEM, XPS, H_2-TPR, and ICP-OES techniques to explore the effects of the methanesulfonic acid (MSA) ligand on the catalytic performance of the zinc catalyst in the hydration of acetylene. It was proved that the MSA ligand was an excellent ligand to improve the catalytic activity of the Zn-based catalyst for the hydration of acetylene. An outstanding catalytic stability was exhibited over the Zn-1.5MSA/MCM-41 catalyst with the C_2H_2 conversion of 99%, and the selectivity to CH_3CHO was above 70% within 150 h. Moreover, the characterization results showed that the addition of the MSA ligand could provide more acid sites and improve the dispersion of the metal catalyst. Moreover, the aggregation of Zn species and the loss of active Zn species were the main reasons for the deactivation of the Zn-based catalyst during the catalytic stability test for acetylene hydration. This study would provide more valuable perspectives for the design of ligand catalysts for the hydration of acetylene.

1. Introduction

Acetaldehyde is an important chemical commodity for the synthesis of many high-value chemicals due to its excellent reactivity.[1,2] Before 1950s, industrial acetaldehyde could be manufactured by acetylene hydration and ethylene oxidation, in which acetylene hydration was an ancient process to prepare acetaldehyde.[3] In early 1881, acetylene hydration was widely used in the industrial production of acetaldehyde in coal-rich countries and regions.[4] At present, combined with China's energy structure, acetylene hydration to acetaldehyde showed some advantages including cost, resources, and technologies.

Previous studies have shown that some transition metal cations (Hg, Ag, Cu, Cd, Pd, and Zn) could be used as active components for acetylene hydration. In fact, many transition metal oxides, molybdates, and cationic zeolites have been found to be active in acetylene hydration.[5–8] Moreover, researchers reported that the cationic zeolite catalysts of cadmium and zinc were not reduced in acetylene hydration as compared to other metals, which showed better activity and stability.[5,6] In recent years, it has been aimed to study Zn-based catalysts for acetylene hydration. For instance, Zn-based catalysts with PEI, APTES, titania, and zirconia modified MCM-41 were prepared and applied to acetylene hydration.[9–12] The modified support enhanced the interaction of metal-support and improved dispersion, thereby effectively improving the performance of the Zn-based catalyst. Moreover, other efforts have also been applied to improve the catalytic stability for acetylene hydration.[13,14] Nevertheless, the catalytic stability of Zn-based catalysts is still the core of the present study stage needed for a breakthrough.

The application of ligand-modified metal catalysts in heterogeneous reactions has attracted extensive attention in recent years.[15–17] Many study results concluded that suitable ligands could be coordinated with metal ions, which would effectively promoted the dispersion of catalysts, inhibited the reduction of metal ions, and reduced the aggregation of catalysts, and thus greatly improved the catalytic performance of the metal catalysts. Hu *et al.* reported that the coordination of the HMPA ligand with Cu can improve the dispersion of Cu species and inhibit the generation of carbon deposition and the loss of Cu species and thereby increase the operation life of the Cu catalyst for acetylene hydrochlorination.[18] In addition, the application of Cu complex catalysts in acetylene hydration has also been reported recently. Zhang *et al.* reported that the Cu-1HEDP/AC catalyst exhibited a high catalytic performance with an initial conversion of 99.7% and selectivity of 92%, while the catalytic stability was only 20 h.[19]

Based on this, we focused on the application of zinc–ligand catalysts for acetylene hydration to obtain a higher catalytic stability. To the best of our knowledge, methanesulfonic acid (MSA) is considered a green organic acid due to low volatility,

School of Chemistry and Chemical Engineering, Shihezi University/State Key Laboratory Incubation Base for Green Processing of Chemical Engineering, Shihezi, Xinjiang, 832000, P. R. China. E-mail: wqq_shzu@sina.com, db_tea@shzu.edu.cn

low toxicity, good biodegradability, and relatively low price.[20] Most importantly, the use of the MSA ligand is in coordination with metals to form coordination compounds. At present, there are no literature reports on the application of zinc–ligand catalysts in the hydration of acetylene. Moreover, catalytic stability is still an urgent problem to be solved in acetylene hydration reactions. Therefore, in this study, a new Zn-based catalyst system with an MSA additive was synthesized, and the catalytic performance for acetylene hydration was evaluated in a micro fixed-bed reactor. All catalysts were characterized by XRD, BET, TGA, TEM, XPS, H_2-TPR, and ICP-OES techniques to explore in detail the effects of the methanesulfonic acid (MSA) ligand on the catalytic performance of the zinc catalyst in the hydration of acetylene. This study would provide more valuable perspectives on the design of ligand catalysts for the hydration of acetylene.

2. Experimental

2.1 Catalyst preparation

All Zn-based catalysts were obtained through wet impregnation. Specifically, the $ZnCl_2$ precursor and MSA ligand were firstly dissolved in 20 mL deionized water, and the mixture was stirred continuously at ambient temperature for 0.5 h until a clear solution was formed. Then, 2 g of MCM-41 support was added to the above clarified solution to obtain a intense mixture. The mixture was continuously stirred for 10 h and the Zn-*x*MSA/MCM-41 catalyst was obtained after the resulting white mixture was dried at 80 °C in a drying cabinet for 24 h. Here, *x* represents the molar ratio of the MSA ligand to $ZnCl_2$ (x = 0.5, 0.75, 1, 1.25, 1.5, and 2). Moreover, the Zn/MCM-41 catalyst with no ligand and MSA/MCM-41 catalyst were prepared by the same method. It is worth noting that the theoretical content of Zn was 7.2 wt% in all Zn-based catalysts.

2.2 Characterization technologies

The texture properties of all samples were measured using a Micrometrics ASAP 2020C Apparatus. To investigate the thermal stability (carbon content) of the catalyst, thermogravimetric (TG) curves were obtained by a SDT Q600 V20.9 Build 20 instrument with a N_2 (air) atmosphere of 100.0 mL min^{-1}. The Fourier transform infrared (FT-IR) spectra of all materials were recorded on a Thermo Fisher Nicolet iS5 instrument to analyze the surface functional groups of catalysts. X-Ray power diffraction (XRD) analysis was conducted on an UltimaIV apparatus to analyze the crystal structure changes of catalysts before and after the reaction. X-Ray photoelectron spectroscopy (XPS) characterization was performed using a Thermo Scientific K-Alpha+ instrument to understand the element state and relative content with the catalyst surface and binding energy was corrected by C 1s (284.6 eV). Transmission electron microscopy (TEM) pictures were acquired on a JEOL JEM2010 equipment tested for 200 kV to find the form of catalysts and the distribution of active substances in the catalysts. The load of Zn in samples was measured through ICP-OES on an Agilent 5110 equipment.

2.3 Evaluation of catalyst performance

The catalytic performance was tested using 2 mL catalyst in a fixed-bed glass microreactor (i. d. of 10 mm) for the hydration of acetylene. Typically, 2 ml of the prepared catalyst was added in the reactor. Before the reaction, the pipeline was cleaned with N_2 for 30 min to remove water and air, and then the reaction tube was heated. After the temperature reached 260 °C, the reaction tube was filled with water vapor for 0.5 h to activate the catalyst. Then, acetylene and water vapor were passed into the reaction tube for reaction to the C_2H_2 GHSV of 90 h^{-1} and the molar ratio of $H_2O:C_2H_2$ = 4 : 1, and finally the reaction products of the residual products were together analysed by gas chromatography. In addition, acetylene conversion (XA) and selectivity to acetaldehyde (SAA) are the performance indicators for the Zn catalyst, and the calculation equation is as follows:

$$X_A = \frac{\Phi_{A0} - \Phi_A}{\Phi_{A0}} \times 100\%$$

$$S_{AA} = \frac{\Phi_A}{1 - \Phi_A} \times 100\%$$

where Φ_{A0} and Φ_A are the volume fraction of the initial and remaining acetylene, respectively.

3. Results and discussion

3.1 Catalytic performance of catalysts

Fig. 1 shows the catalytic performance with all Zn-based catalysts having different $ZnCl_2$/MSA molar ratios for acetylene hydration. The tested results revealed that acetylene conversion decreased from 92% to 68% and the selectivity to acetaldehyde reduced by 13% for the Zn/MCM-41 catalyst after 10 h of reaction, which indicated that the Zn/MCM-41 catalyst showed worse catalytic stability. However, it could be seen from Fig. 1 that the selectivity to acetaldehyde of all Zn-*x*MSA/MCM-41 catalysts remained unchanged within 10 h of reaction, and the acetylene conversion decreased more slowly compared with the Zn/MCM-41 catalyst. In particular, the outstanding catalytic performance was observed in the Zn-1.5MSA/MCM-41 catalyst.

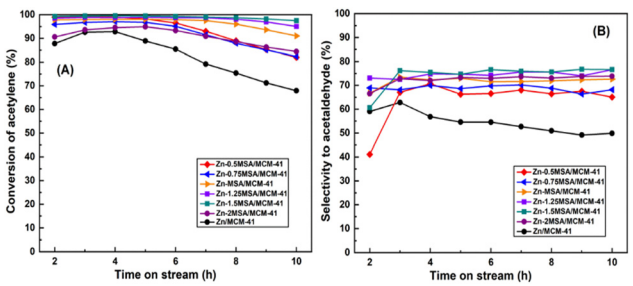

Fig. 1 Acetylene conversion (A) and selectivity to acetaldehyde (B) of the catalysts in acetylene hydration.

The conversion of acetylene decreased by 2% from 99% within 10 h, and the selectivity to acetaldehyde remained about 76%. Therefore, it could be concluded that the activity of the Zn-based catalyst for the hydration of acetylene greatly improved by adding the MSA ligand and the optimal $ZnCl_2$/MSA molar ratio was 1 : 1.5.

Furthermore, the catalytic stability of the Zn-1.5MSA/MCM-41 catalyst for acetylene hydration was further proved by the operation of the catalyst for 150 h. As shown in Fig. 2, within 70 h, the selectivity to acetaldehyde was still about 74%, and the conversion of acetylene was above 90%. After 150 h of reaction, the selectivity was reduced to 70%, and the conversion was reduced to 78%, indicating that the addition of MSA ligand effectively reduced the catalyst deactivation rate of the Zn-based catalyst. This inference also indicates that the results of the study are in accordance with our desired goal to improve the stability of the catalyst by adding a ligand. Importantly, the catalytic stability of the Zn-1.5MSA/MCM-41 catalyst is the longest catalytic stability test data reported in the hydration of acetylene reaction at present.

3.2 FT-IR characterization

Fourier transform infrared spectroscopy (FT-IR) characterization was used to ascertain the characteristic functional groups of the MCM-41 support, pure MSA ligand, and Zn-*x*MSA/MCM-41 catalysts. As shown in Fig. 3, the spectra of fresh Zn/MCM-41, Zn-1.5MSA/MCM-41, MSA/MCM-41, and MCM-41 samples were in unanimity.[21] The spectra at 3400 cm^{-1} and 1627 cm^{-1} corresponded to the –OH group of adsorbed water on the material surface. The spectra at 1235 cm^{-1} and 1082 cm^{-1} could be due to the asymmetric vibration of Si–O–Si functional groups, while the peak at 797 cm^{-1} corresponded to the symmetric stretching vibration of Si–O–Si in MCM-41. The Si–O–H stretching vibration of the support was observed at 965 cm^{-1}. In addition, Zn/MCM-41 and Zn-1.5MSA/MCM-41 catalysts showed a small band at 1400 cm^{-1}, in the plane bending vibration of –OH, which was related to the water absorption of $ZnCl_2$.[22] On the other hand, according to the methanesulfonic acid complex studies in the literature,[23,24] the

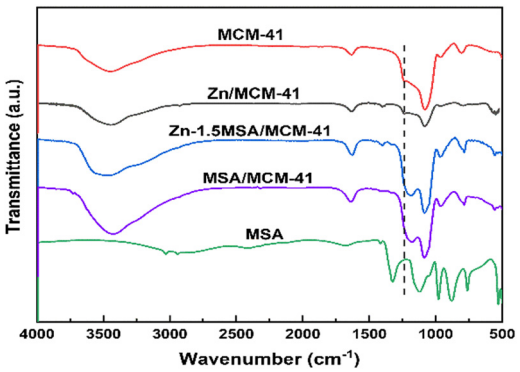

Fig. 3 FT-IR spectra of fresh catalysts.

absorption at 763 cm^{-1} corresponded to the stretching vibration of C–S, and the spectra at 1126 cm^{-1} and 1049 cm^{-1} were asymmetric and symmetric stretching vibrations of $–SO_2–$, respectively, but it was difficult to determine whether MSA existed in catalysts because the bands of the MSA ligand in the range of 500–2000 cm^{-1} coincided with that of the MCM-41 carrier. Nevertheless, the Zn-1.5MSA/MCM-41 catalyst and the MSA/MCM-41 catalyst showed absorption peaks at 1194 cm^{-1} and 1176 cm^{-1}, respectively, with a disappearance of the peak at 1235 cm^{-1}, which indicated that MSA was introduced into the support, and the peak blue shifted from 1176 cm^{-1} to 1194 cm^{-1} in the Zn-1.5MSA/MCM-41 catalyst compared with MSA/MCM-41.

3.3 TG characterization

The TG results of catalysts are shown in Fig. 4, which were tested in an N_2 atmosphere to confirm the thermal stability of Zn/MCM-41, Zn-1.5MSA/MCM-41, and MSA/MCM-41 catalysts during the reaction. The Zn/MCM-41 and Zn-1.5MSA/MCM-41 catalysts had similar weight loss before 325 °C, which could be considered as the volatilization of adsorbed water on the catalyst surface (<150 °C) and the decomposition of a small fraction of Zn species (150–325 °C). While a significant difference in the weight loss between the two catalysts in 325–500 °C was observed. The results showed that the Zn-1.5MSA/MCM-41

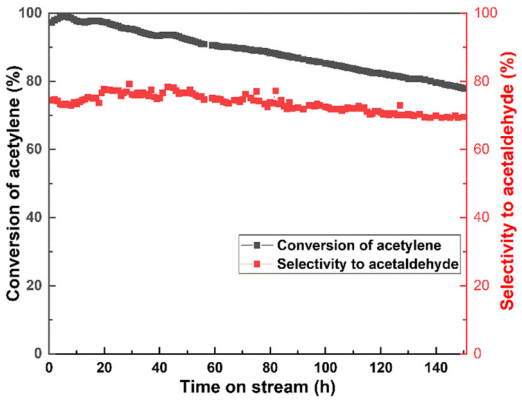

Fig. 2 Catalytic stability test of the Zn-1.5MSA/MCM-41 catalyst in acetylene hydration.

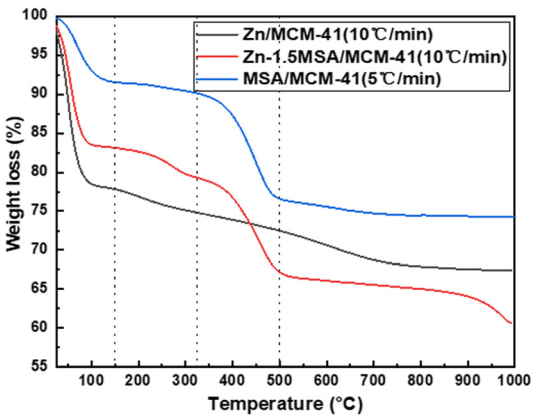

Fig. 4 TG curves of the fresh catalysts.

catalyst and the MSA/MCM-41 catalyst had large weight loss in the temperature range of 325–500 °C, which was probably due to the decomposition of the MSA ligand. This indicated that the prepared Zn-1.5MSA/MCM-41 catalyst had good thermal stability and would not decompose at the reaction temperature of acetylene hydration.

3.4 BET characterization

The texture properties and N_2 adsorption–desorption isotherms of all catalysts are shown in Table 1 and Fig. 5. It could be seen from Table 1 that the specific surface area and pore volume of the catalyst diminished with the addition of MSA ligand, which was attributed to the entry of catalyst particles into the pore channel of the support. Compared with the isotherms of all catalysts, it was found that there was a hysteresis loop between P/P_0 = 0.4–1.0, implying the mesoporous structural property of the carrier,[25] which meant that the mesoporous property of the support has been retained after the addition of MSA and reaction for 10 h.

3.5 XRD characterization

Wide angle XRD characterization over the fresh and used catalysts was used to investigate the change in the crystal phase structure of the catalysts. Both catalysts displayed a wide characteristic peak at about 23° in Fig. 6(A), corresponding to amorphous silica in the MCM-41 mesoporous molecular sieve.[26] No diffraction peaks of Zn species or MSA ligand were observed, which implied that the Zn active species were well dispersed on the support, or the Zn species along with the MSA ligand existed in amorphous forms. In addition, small angle XRD was used to determine the ordered structure of MCM-41 support, as shown in Fig. 6(B). The long-range ordering of the MCM-41 carrier in Zn/MCM-41 catalysts before and after the reaction were determined by three well-defined peaks located at 2.3°, 3.8°, and 4.6°, which corresponded to the (1 0 0), (1 1 0), and (2 0 0) planes of the ordered hexagonal channel structure of MCM-41, respectively.[27] However, the diffraction peaks almost disappeared after the addition of MSA ligand, which may be due to the catalyst particles entering into the pores of MCM-41, resulting in the severe disintegration of the ordered mesoporous structure of the support.

3.6 Surface morphologies of the catalysts

As we all know, the uniform dispersion of active metal substances is of great importance to the stability of the catalysts. Therefore, in order to observe the dispersion of the catalyst before and after the reaction, TEM characterization was performed. As shown in Fig. 7, there are no active component particles on the surface of all fresh catalysts, which may be due to the better dispersion of active species or smaller particle size. Nevertheless, the spent Zn/MCM-41 catalyst showed certain agglomeration, while no particle agglomeration was observed in the spent Zn-1.5MSA/MCM-41 catalyst, indicating that the addition of MSA could inhibit the agglomeration of catalyst

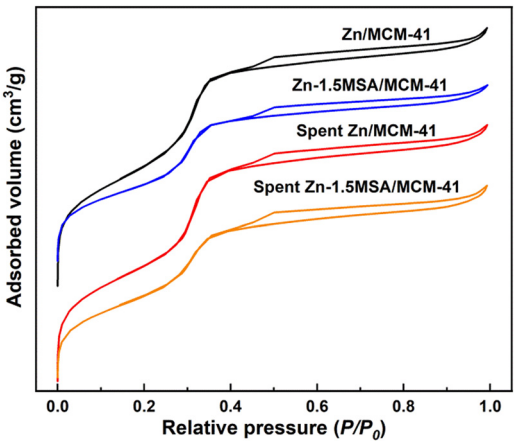

Fig. 5 N_2 adsorption isotherms of fresh and spent catalysts.

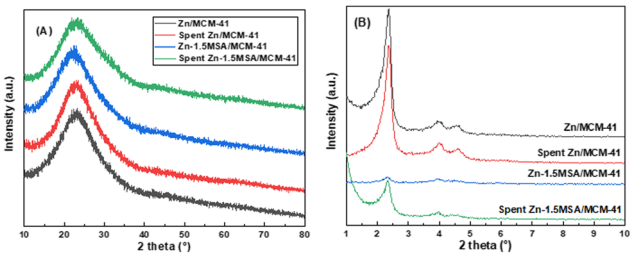

Fig. 6 Wide angle XRD patterns (A) and small angle XRD patterns (B) of the fresh and used catalysts.

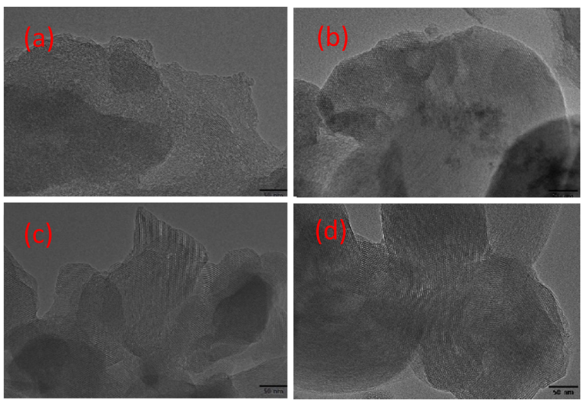

Fig. 7 TEM images of fresh Zn/MCM-41 (a), Zn-1.5 MSA/MCM-41 (c), spent Zn/MCM-41 (b), and spent Zn-1.5 MSA/MCM-41 (d) catalysts.

Table 1 The content of Zn and texture properties of fresh and used catalysts

Samples	S_{BET} ($m^2\ g^{-1}$)	V ($cm^3\ g^{-1}$)	D (nm)
Zn/MCM-41	788.2	0.7	3.4
Spent Zn/MCM-41	755.3	0.7	3.5
Zn-1.5MSA/MCM-41	527.7	0.5	3.5
Spent Zn-1.5MSA/MCM-41	567.5	0.5	3.6
Spent Zn-1.5MSA/MCM-41(150 h)	539.0	0.5	4.0

particles to certain extent. Therefore, the Zn-1.5MSA/MCM-41 catalyst showed better stability than the Zn/MCM-41 catalyst.

3.7 XPS characterization

Fig. 8 shows the XPS pattern of Zn $2p_{3/2}$ in the fresh and spent Zn/MCM-41 and Zn-1.5 MSA/MCM-41 catalysts. As shown in the figure, the binding energy of Zn shifted slightly to the lower part of the spectra after adding the MSA ligand, which indicated that Zn acquired electrons from MSA, thus, increasing the electron cloud density around the Zn active component. All the catalysts showed two states of existence, with $(ZnOH)^+$ species at high binding energy and $(ZnH)^+$ species at low binding energy.[28,29] The relative content of Zn species in all catalysts is shown in Table 2. It could be found that there were more $(ZnOH)^+$ species in the fresh Zn-1.5MSA/MCM-41 catalysts. Moreover, the relative content of $(ZnOH)^+$ species in the Zn-1.5MSA/MCM-41 catalyst decreased significantly less than that of Zn/MCM-41 catalyst after 10 h of reaction. Higher electron cloud density of the Zn active species and more $(ZnOH)^+$ species contributed to the catalytic reaction. In addition, ICP-OES characterization was used to evaluate the load of Zn in the catalysts, and the results are shown in Table 2. The loading of Zn species in the two fresh catalysts was similar to the theoretical content, and it could be seen the Zn content in the spent catalysts decreased slightly. Further, the MSA ligand inhibited the loss of Zn to some extent, which could improve the catalytic activity of the Zn-based catalyst in the hydration of acetylene.

3.8 Py-FTIR characterization

As far as we know, the surface acidity of the catalyst has certain impact on the performance of the catalyst, and MSA is a strong organic acid; thus, it was speculated that the addition of MSA might change the surface acid properties of the catalyst. Therefore, in order to further understand the acid content and distribution of acid sites, the Py-FTIR (as shown in Fig. 9) characterization was carried out for the MCM-41 support, Zn/MCM-41 catalyst, 1.5MSA/MCM-41 catalyst, and Zn-1.5MSA/MCM-41 catalyst. The spectra at 1445 cm^{-1} and 1545 cm^{-1} were attributed to pyridine adsorbed at Lewis acid sites and

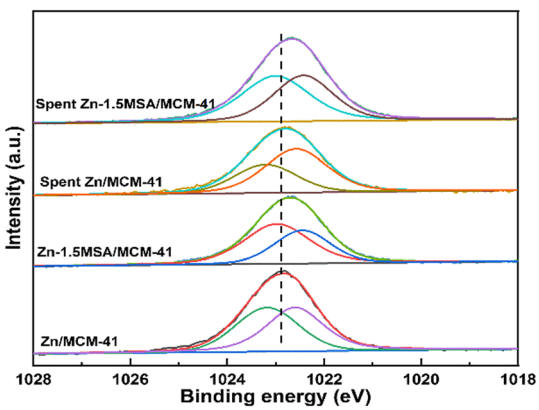

Fig. 8 Zn $2p_{3/2}$ XPS pattern of the fresh and used catalysts.

Table 2 Composition of Zn on the catalyst surface

	Binding energy (eV)				Zn (wt%)
Samples	$(ZnH)^+$	$(ZnOH)^+$	$(ZnOH)^+$ (%)	$(ZnH)^+$ (%)	—
Zn/MCM-41	1022.6	1023.2	48.4	51.6	7.47
Spent Zn/MCM-41	1022.6	1023.2	37.6	62.4	7.22
Zn-1.5MSA/MCM-41	1022.5	1023.0	60.2	39.8	6.29
Spent Zn-1.5 MSA/MCM-41	1022.4	1023.0	54.4	45.6	6.14

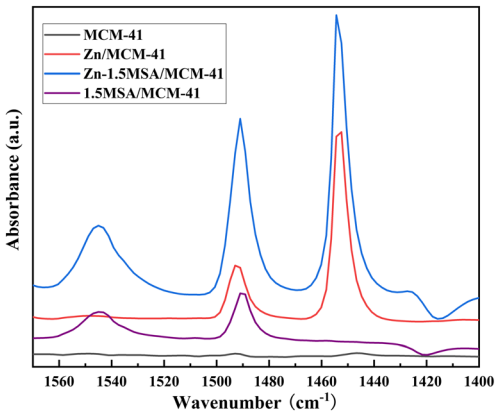

Fig. 9 Py-FTIR spectra of the catalysts.

Brønsted acid sites, respectively, while the spectrum at 1490 cm^{-1} is attributed to pyridine adsorbed at both Lewis and Brønsted acid sites in the Py-FTIR spectra.[29,30] As shown in Fig. 9, it is clearly shown that there is no MCM-41 absorption peak; it is a fact that pure MCM-41 exhibits almost no acidity.[31,32] The absorption peak of the Zn/MCM-41 catalyst at about 1450 cm^{-1} indicates that it is a Lewis acid solid catalyst. The spectra at 1545 cm^{-1} and 1490 cm^{-1} for the 1.5MSA/MCM-41 catalyst suggest that it is a Brønsted acid catalyst. Therefore, it was speculated that the increase in acid sites as well as the coordination between Lewis and Brønsted acid sites might be another reason for the improvement of the Zn-1.5MSA/MCM-41 catalyst catalytic performance. Although the acid site could promote acetylene hydration to a certain extent, the acid site was also the active site for the aldol condensation reaction,[33] which also explains that the addition of MSA ligand in the Zn-based catalyst improved the catalytic performance and stability of the catalyst, while the selectivity to acetaldehyde was still not ideal.

3.9 Catalyst deactivation

In addition, the reasons of catalyst deactivation for the Zn-1.5MSA/MCM-41 catalyst were preliminarily explored for acetylene hydration. The TEM images (Fig. 10) of the spent Zn-1.5MSA/MCM-41 catalyst showed that the catalyst particles had clear accumulation after 150 h of reaction. In addition, carbon deposition during the reaction was estimated by calculating the weight difference between the fresh and spent catalysts in the

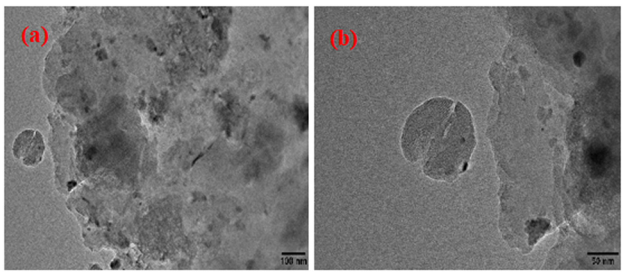

Fig. 10 TEM images of the spent Zn-1.5MSA/MCM-41(150 h) catalyst.

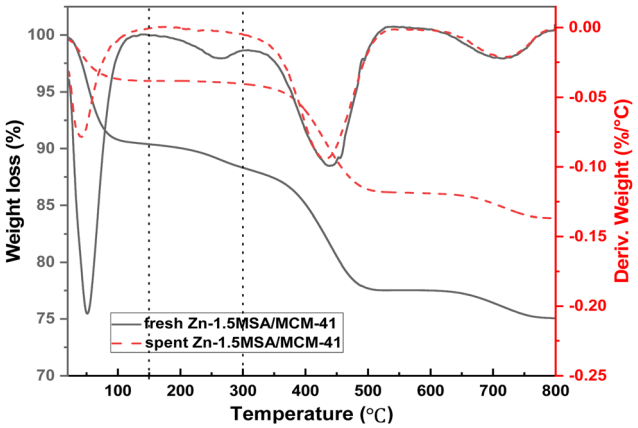

Fig. 11 TG-DTG curves of fresh and spent Zn-1.5MSA/MCM-41 catalysts.

same temperature range (150–300 °C). From the TG curve in Fig. 11, it can be seen that compared with the used catalyst, the mass loss of the fresh catalyst in the temperature range of 150–300 °C is more, which is due to the decomposition of some active components in the reaction process, while the used catalyst basically has no mass loss, which indicates that there is almost no carbon deposition even after 150 h of reaction. Moreover, after 150 h of reaction, the specific surface area of the catalyst was 539 m^2 g^{-1}, the pore volume was 0.5 cm^2 g^{-1}, and the pore diameter was 4.0 nm. Compared with fresh catalysts (as shown in Table 1), the texture structure changed slightly, which also indicated that there was no large amount of carbon deposition during the reaction. It is revealed that the high stability of the Zn-1.5MSA/MCM-41 catalyst is closely related to its good resistance to carbon deposition. Moreover, the content of Zn in the catalyst decreased from 6.90% to 5.46% after 150 h of reaction and about 20.9% of Zn species was lost. Therefore, it was concluded that the agglomeration and the loss of Zn species of the catalyst were the main reasons of catalyst deactivation in the hydration of acetylene.

4. Conclusions

In this study, a new Zn-based catalyst system with an MSA additive was synthesized, and the catalytic performance for acetylene hydration was evaluated in a micro fixed-bed reactor. The performance test results showed that the Zn-1.5MSA/MCM-41 catalyst exhibited excellent catalytic performance and stability with about 80% acetylene conversion, and the selectivity of acetaldehyde decreased by about 8% only after 150 h of operation. The improvement of the catalyst performance could be attributed to the increase in the acid content, decrease in the agglomeration of active components, and higher electron cloud density around the Zn species after the addition of MSA. In addition, the excellent carbon deposition resistance also contributed to the outstanding stability of the Zn-1.5MSA/MCM-41 catalyst. Moreover, the aggregation of Zn species and the loss of active Zn species were the main reasons for Zn-based catalyst deactivation during the catalytic stability tests for the acetylene hydration reaction. This study would provide a high reference value for the development and preparation of efficient and stable catalysts for acetylene hydration.

Author contributions

Bin Dai and Qinqin Wang designed the experiments. Sudi Zhang and Zhen Chen prepared samples, carried out characterization and tested the catalytic performance. Sudi Zhang and Qinqin Wang contributed to the analysis and discussion of the results. Sudi Zhang, Qinqin Wang and Bin Dai wrote the paper. All authors discussed the results and commented on the manuscript.

Conflicts of interest

There are no conflicts to declare.

Acknowledgements

We gratefully acknowledge the financial support provided by the High-level Talent Scientific Research Project of Shihezi University (No. RCZK201934, No. SHYL-BQ201906) and the National Natural Science Funds of China (NSFC, 22178225).

References

1 A. S. Hester and K. Himmler, Staff-industry collaborative report chemicals from acetaldehyde, *Ind. Eng. Chem.*, 1959, **51**, 1424–1430.
2 H. A. Wittcoff, Acetaldehyde: a chemical whose fortunes have changed, *J. Chem. Educ.*, 1983, **60**, 1044–1047.
3 I. T. Trotuş, T. Zimmermann and F. Schüth, Catalytic reactions of acetylene: A feedstock for the chemical industry revisited, *Chem. Rev.*, 2014, **114**, 1761–1782.
4 D. A. Ponomarev and S. M. Shevchenko, Hydration of acetylene: A 125th anniversary, *J. Chem. Educ.*, 2007, **84**, 1725–1726.
5 P. Moggi and G. Albanesi, Transition metal phosphomolybdates as catalysts for the gas phase hydration of acetylene to acetaldehyde and acetic acid, *React. Kinet. Catal. Lett.*, 1991, **44**, 375–380.

6 G. Onyestyák and D. Kalló, Interactions of reactants in hydration of acetylene on Cd-zeolite catalysts, *J. Mol. Catal. A: Chem.*, 1996, **106**, 103–108.
7 D. Kalló and G. Onyestyák, Deactivation and stabilization of late transition metal zeolite catalysts for acetylene hydration, *Stud. Surf. Sci. Catal.*, 1987, **34**, 605–612.
8 G. Onyestyák and D. Kalló, Hydration of acetylene on Zn and Cd-zeolites, *Microporous Mesoporous Mater.*, 2003, **61**, 199–204.
9 Q. Wang, M. Zhu, B. Dai and J. Zhang, A novel and effective Zn/PEI-MCM catalyst for the acetylene hydration to acetaldehyde, *Chin. Chem. Lett.*, 2019, **30**, 1244–1248.
10 Q. Q. Wang, M. Y. Zhu and H. Y. Zhang, *et al.*, Highly Active Amino-Modified MCM-41-Supported Zinc Catalyst for Acetylene Hydration to Acetaldehyde, *ChemistrySelect*, 2018, **3**(33), 9603–9609.
11 Q. Wang, M. Zhu and B. Dai, *et al.*, Zn supported on titania-doped mesoporous silicate MCM-41 as efficient catalysts for acetylene hydration, *Catal. Sci. Technol.*, 2019, **9**(4), 981–991.
12 Q. Wang, B. Dai and J. Zhang, Catalytic Acetylene Hydration over the Zn/Zr-MCM Catalyst: Effect of preparation methods for doping zirconia on catalytic performance, *Appl. Catal., A*, 2022, 118476.
13 Q. Wang, M. Zhu and H. Zhang, *et al.*, Enhanced catalytic performance of Zr-modified ZSM-5-supported Zn for the hydration of acetylene to acetaldehyde, *Catal. Commun.*, 2019, **120**, 33–37.
14 Q. Wang, M. Zhu and C. Xu, *et al.*, Zn–Cu bimetallic catalysts supported on pure silica MCM-41 for acetylene hydration reaction, *New J. Chem.*, 2018, **42**(8), 6507–6514.
15 Y. Dong, W. Li, Z. Yan and J. Zhang, Hydrochlorination of acetylene catalyzed by an activated carbon supported chlorotriphenylphosphine gold complex, *Catal. Sci. Technol.*, 2016, **6**, 7946–7955.
16 H. Li, B. Wu, F. Wang and X. Zhang, Achieving Efficient and Low Content Ru-Based Catalyst for Acetylene Hydrochlorination Based on N,N'-Dimethylpropyleneurea, *ChemCatChem*, 2018, **10**, 4090–4099.
17 X. Wang, M. Zhu and B. Dai, Effect of Phosphorus Ligand on Cu-Based Catalysts for Acetylene Hydrochlorination, *ACS Sustainable Chem. Eng.*, 2019, **7**, 6170–6177.
18 Y. Hu, Y. Wang and Y. Wang, *et al.*, High performance of supported Cu-based catalysts modulated via phosphamide coordination in acetylene hydrochlorination, *Appl. Catal., A*, 2020, **591**, 117408.
19 Qiang Zhang, Xiaohong Liu and Jiannan Luo, *et al.*, Complexation effect of copper(ii) with HEDP supported by activated carbon and influence on acetylene hydration, *New J. Chem.*, 2021, **45**, 1712–1720.
20 M. D. Gernon, M. Wu, T. Buszta and P. Janney, Environmental benefits of methanesulfonic acid: Comparative properties and advantages, *Green Chem.*, 1999, **1**, 127–140.
21 M. S. Yılmaz, Ö. D. Özdemir and S. Pişkin, Synthesis and characterization of MCM-41 with different methods and adsorption of Sr^{2+} on MCM-41, *Res. Chem. Intermed.*, 2015, **41**, 199–211.
22 A. Moezzi, M. Cortie and A. McDonagh, Transformation of zinc hydroxide chloride monohydrate to crystalline zinc oxide, *Dalton Trans.*, 2016, **45**, 7385–7390.
23 M. Wang, H. Jiang and Z. C. Wang, Dehydration studies of Co(II), Cu(II) and Zn(II) methanesulfonates, *J. Therm. Anal. Calorim.*, 2006, **85**, 751–754.
24 M. Wang, Z. G. Song, H. Jiang and H. Gong, Thermal decomposition of metal methanesulfonates in air, *J. Therm. Anal. Calorim.*, 2009, **98**, 801–806.
25 M. Kruk, M. Jaroniec and A. Sayari, Adsorption Study of Surface and Structural Properties of MCM-41 Materials of Different Pore Sizes, *J. Phys. Chem. B*, 1997, **5647**, 583–589.
26 M. Popova, Á. Szegedi, Z. Cherkezova-zheleva, I. Mitov, N. Kostova and T. Tsoncheva, Toluene oxidation on titanium- and iron-modified MCM-41 materials, *J. Hazard. Mater.*, 2009, **168**, 226–232.
27 D. Liu, G. Li, H. Guo and J. Liu, Facile preparation of bifunctional iron doped mesoporous materials and their application in the cycloaddition of CO_2, *J. Energy Chem.*, 2020, **41**, 52–59.
28 S. Tamiyakul, T. Sooknoi, L. L. Lobban and S. Jongpatiwut, Generation of reductive Zn species over Zn/HZSM-5 catalysts for n-pentane aromatization, *Appl. Catal., A*, 2016, **525**, 190–196.
29 X. Niu, J. Gao, Q. Miao, M. Dong, G. Wang, W. Fan, Z. Qin and J. Wang, Influence of preparation method on the performance of Zn-containing HZSM-5 catalysts in methanol-to-aromatics, *Microporous Mesoporous Mater.*, 2014, **197**, 252–261.
30 E. Modrogan, M. H. Valkenberg and W. F. Hoelderich, Phenol alkylation with isobutene-influence of heterogeneous Lewis and/or Brønsted acid sites, *J. Catal.*, 2009, **261**, 177–187.
31 A. Matsumoto, H. Chen, K. Tsutsumi, M. Grün and K. Unger, Novel route in the synthesis of MCM-41 containing framework aluminum and its characterization, *Microporous Mesoporous Mater.*, 1999, **32**, 55–62.
32 K. Y. Kwak, M. S. Kim, D. W. Lee, Y. H. Cho, J. Han, T. S. Kwon and K. Y. Lee, Synthesis of cyclopentadiene trimer (tricyclopentadiene) over zeolites and Al-MCM-41: The effects of pore size and acidity, *Fuel*, 2014, **137**, 230–236.
33 Z. D. Young, S. Hanspal and R. J. Davis, Aldol Condensation of Acetaldehyde over Titania, Hydroxyapatite, and Magnesia, *ACS Catal.*, 2016, **6**, 3193–3202.